HHS Public Access

Author manuscript

Cell Rep. Author manuscript; available in PMC 2020 February 19.

Published in final edited form as:

Cell Rep. 2019 December 17; 29(12): 4186–4199.e3. doi:10.1016/j.celrep.2019.11.051.

The *Arabidopsis* Transcriptome Responds Specifically and Dynamically to High Light Stress

Jianyan Huang[1,2,4], **Xiaobo Zhao**[1,2,3,4,*], **Joanne Chory**[1,2,5,*]

[1]Howard Hughes Medical Institute, Salk Institute for Biological Studies, La Jolla, CA 92037, USA

[2]Plant Biology Laboratory, Salk Institute for Biological Studies, La Jolla, CA 92037, USA

[3]Institute of Nuclear Agricultural Sciences, Key Laboratory of Nuclear Agricultural Sciences of Ministry of Agriculture and Zhejiang Province, College of Agriculture and Biotechnology, Zhejiang University, Hangzhou 310058, China

[4]These authors contributed equally

[5]Lead Contact

SUMMARY

The dynamic and specific transcriptome for high light (HL) stress in plants is poorly understood because heat has confounded previous studies. Here, we perform an in-depth temporal responsive transcriptome analysis and identify the core HL-responsive genes. By eliminating the effect of heat, we uncover a set of genes specifically regulated by high-intensity light-driven signaling. We find that 79% of HL-responsive genes restore their expression to baseline within a 14-h recovery period. Our study reveals that plants respond to HL through dynamic regulation of hormones, particularly abscisic acid (ABA), photosynthesis, and phenylpropanoid pathway genes. Blue/UV-A photoreceptors and phytochrome-interacting factor (*PIF*) genes are also responsive to HL. We further show that ABA biosynthesis-defective mutant *nced3nced5*, as well as *pif4*, *pif5*, *pif4*,*5*, and *pif1*,*3*,*4*,*5* mutants, are hypersensitive to HL. Our study presents the dynamic and specific high-intensity light-driven transcriptional landscape in plants during HL stress.

Graphical Abstract

*Correspondence: xbzhao@zju.edu.cn (X.Z.), chory@salk.edu (J.C.).

AUTHOR CONTRIBUTIONS

J.H., X.Z., and J.C. designed the research; J.H. and X.Z. performed the research and analyzed the data; J.H., X.Z., and J.C. wrote the manuscript.

DECLARATION OF INTERESTS

The authors declare no competing interests.

SUPPLEMENTAL INFORMATION

Supplemental Information can be found online at https://doi.org/10.1016/j.celrep.2019.11.051.

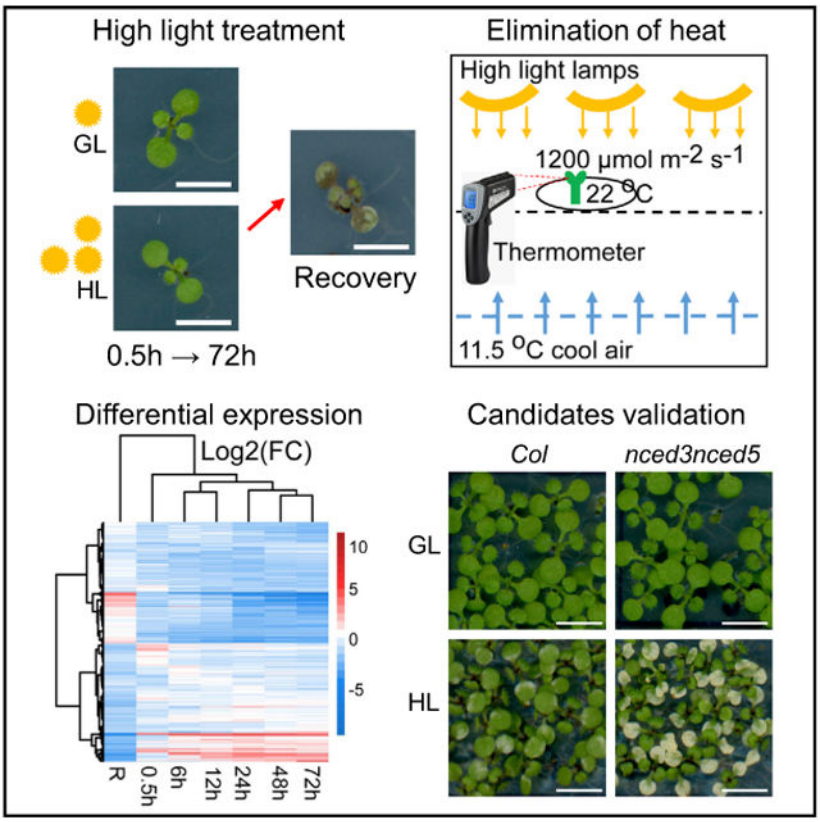

In Brief

Huang et al. present the specific and dynamic transcriptome for high-intensity light (HL) stress in plants. They identify the core HL-responsive genes and uncover that plants respond to HL by dynamically regulating hormones, anthocyanin, photosynthesis, photoreceptors, and *PIF* genes. They show that ABA and PIFs are required for HL response.

INTRODUCTION

Being sessile organisms, plants have evolved sophisticated acclimation and defense mechanisms to cope with different challenges in their environment. Light is the most rapidly changing and variable environmental factor for plant photoautotrophic lifestyle, but it is also the most important, because it provides the source of energy for photosynthesis and plays a key role in multiple plant developmental processes (Jiao et al., 2007; Kaiserli et al., 2015). However, during most days of the life cycle, plants encounter high light (HL) intensity that exceeds their photosynthetic capacity (Mishra et al., 2012). The exposure of plants to high-intensity light that exceeds the energetic demand of the plants or their capacity to dissipate the excessive light energy may cause a range of HL stress responses. Protection against excess absorbed energy under HL involves rapid-response mechanisms like non-photochemical energy quenching (NPQ) (Goss and Lepetit, 2015; Ruban, 2016). NPQ dissipates excess excitation energy as heat and is broadly considered a major factor in the rapid regulation of light harvesting to protect the Photosystem II reaction centers against

photodamage that leads to photoinhibition of photosynthesis (Ruban, 2016). HL stress ultimately causes the accumulation of multiple reactive oxygen species (ROS), including hydrogen peroxide (H_2O_2), superoxide (O_2^-), and singlet oxygen ($^1O_2$) that can both signal and cause damage (Apel and Hirt, 2004). Plants have developed various acclimation processes to cope with long-term HL stress through both optimizing energy use and avoiding damage caused by HL, including variations in the composition of the photosynthetic apparatus (Walters, 2005; Schöttler and Tóth, 2014), changing chloroplast and leaf avoidance movements (Kasahara et al., 2002; Wada, 2013), leaf morphology (Kim et al., 2005), and leaf optics (Knapp and Carter, 1998).

Regulation of gene expression is an important aspect of response and acclimation to HL stress. It has been demonstrated that HL leads to transcriptional suppression of genes encoding antenna proteins and transcriptional activation of genes encoding enzymes responsible for ROS scavenging (Rossel et al., 2002; Kleine et al., 2007; Jung et al., 2013). Previous studies showed that the transcriptional response of *Arabidopsis* to HL was triggered within a few seconds or minutes (Vogel et al., 2014; Suzuki et al., 2015) and HL stress-regulated mRNAs exhibited rapid recovery (Crisp et al., 2017). Transcriptional regulatory networks have a key role in mediating light signaling through the coordinated activation and repression of specific downstream genes (Jiao et al., 2007). However, most previous studies either did not consider the effect of temperature increase in HL treatment that could cause heat stress or analyzed HL stress combined with heat stress. For example, many heat stress-related genes, e.g., heat shock protein (*HSP*) genes, have been identified as HL-responsive genes, but it cannot be distinguished whether the differential expression of these genes is driven by high-intensity light, heat, or both. Therefore, the light-driven signaling-associated transcriptional regulation networks under high-intensity light is not well understood.

In nature, HL and heat are not always companions. For example, during winter in the temperate zone or during summer in high-altitude areas (e.g., high mountain regions) or high-latitude areas (e.g., the Arctic Circle area) on Earth, plants experience long exposure to high-intensity light and a cool ambient temperature. Relevant studies showed that in midsummer, the sunlight intensity of the Arctic Circle area could exceed 1,200 μmol m^{-2} s^{-1} and the mean temperature was around 10°C (Wookey et al., 1993). In these conditions, the high-intensity light-driven, but not the heat-driven, signaling pathways may play a unique role in the development, growth, and stress response of plants. Moreover, previous studies were mainly focused on a few short time periods and thus failed to capture the dynamic and genome-wide landscape of responses triggered by middle- and long-term HL stress and recovery from HL stress.

In this study, we aimed to isolate the high-intensity light-driven signaling pathway from high light/heat-combined regulatory networks to discern the specific action and biological consequences of the high-intensity light-driven stress response. In addition, by coupling this isolation with a detailed time course experiment and analyzing the short-, middle-, and long-term responses to HL and recovery, we generated a comprehensive and integrated dataset that provides insight into the complex molecular response of *Arabidopsis* to HL stress and

thereby revealed the potential important regulators and responsive genes for high-intensity light stress in plants.

RESULTS

Experimental Design of High Light and Recovery Treatments

To capture the dynamic transcriptional response of *Arabidopsis* plants to HL stress and recovery, we performed a time course RNA sequencing (RNA-seq) study. *Arabidopsis* seedlings were treated with high light (HL: 1,200 μmol m^{-2} s^{-1}, leaf temperature: 22°C) for 0.5, 6, 12, 24, 48, and 72 h with corresponding growth light (GL: 60 μmol m^{-2} s^{-1}, leaf temperature: 22°C) treatments as control. We also collected the recovery (R) samples (Figure 1A). To avoid stress memory, we used continuous light conditions. The spectrum of HL is shown in Figure 1B. In HL treatment, the light lamps are located at the top of the chamber and the cool air comes from the bottom. By changing the settings, we were able to maintain the temperature of the growth medium and leaf to match the control conditions (Figure 1C). To investigate the light intensity and leaf temperature during winter in the temperate zone in nature, we monitored the light intensity and plant leaf temperature around the Salk Institute for Biological Studies (coordinates: 32.887579° N, −117.244914° W). We found that for most of the day, the light intensity was more than 1,000 μmol m^{-2} s^{-1} and the leaf temperature was between 22°C and 25°C (Figure 1D), which suggested that in nature, plants could be exposed to high-intensity light with no accompanying heat stress. A preliminary experiment indicated that when the chamber was set to 22°C, under 1,200 μmol m^{-2} s^{-1} of HL, the leaf temperature rose to 28°C in 5 min, 32°C in 10 min, and 35°C in 30 min, which would generate heat stress on plants (Figure 1E). By setting the chamber to 11.5°C, the temperature of the medium and leaf was maintained at the normal growth temperature (22°C) (Figure 1E). Similar experimental settings have been employed to avoid leaf heating under HL in previous studies (Ramel et al., 2013). Thus, we excluded the effect of heat from our study.

We confirmed that the HL treatment was successful by examining the induction of HL marker genes. Consistent with previous studies (Casazza et al., 2005; Heddad et al., 2006), we found that *ELIP1* and *ELIP2* had low expression levels under GL and were highly induced by HL (Figure 1F). However, the expression of *APX2* was only slightly upregulated under our HL treatment (Figure 1F). Previous studies showed that *APX2* was highly induced by warm HL(Jung et al., 2013; Crisp et al., 2017). We inferred that *APX2* mainly responded to heat or HL/heat-combined stresses. Thus, we examined the expression of *ELIP1*, *ELIP2*, and *APX2* under HL and warm HL. The results showed that *ELIP1* and *ELIP2* were strongly upregulated by HL and moderately upregulated by warm HL. However, *APX2* was only highly induced by warm HL (Figure 1G), suggesting that *APX2* induction was primarily heat driven, but not light driven. These results emphasize one of the important aspects of our study design: separation of heat from HL to unravel the independent action and biological consequences of a high-intensity light-driven response.

Dynamic Transcriptome Responses of Plants to Short-, Middle-, and Long-Term HL

We used pairwise comparisons (e.g., 0.5 h of HL [HL0.5h] versus 0.5 h of GL [GL0.5h]) to identify differentially expressed genes (DEGs) of each time point. The average reads per kilobase of transcript per million mapped reads (RPKM) of each gene at all time points are listed in Table S1. In total, 5,403 DEGs were identified for at least one time point of HL (Table S2). In detail, there were 1,300 DEGs for 0.5 h, 1,780 DEGs for 6h, 2,021 DEGs for 12 h, 3,081 DEGs for 24 h, 2,681 DEGs for 48 h, and 2,885 DEGs for 72 h (Figure 2A). The recovery sample had 2,156 DEGs compared with 72 h of HL (HL72h) and only had 604 DEGs compared with 72 h of GL (GL72h) (Figure 2A). The expression profiles of all DEGs fell into significant short-term (0.5 h), middle-term (6 to 12 h), and long-term (more than 24 h) HL response patterns (Figure 2B). *cis*-element analysis showed that at most time points, the G box (CACGTG) was significantly enriched in the promoters of DEGs (Figure 2C). We identified nine significant expression clusters from all DEGs in response to different durations of HL, which includes two main clusters: gradually downregulated (1,227 genes) and gradually upregulated (560 genes) (Figure 2D; Table S3). *GPT2*, required for dynamic acclimation of photosynthetic capacity to increase light (Athanasiou et al., 2010), was in cluster 31 (Figure S1A). *MAPKKK18*, which was upregulated by HL (Ramel et al., 2013), was in cluster 33 (Figure S1A). *ERF6* displayed significant upregulation at 10 and 30 min after the low light to HL shift, followed by a strong decline (Vogel et al., 2014). A similar expression pattern was observed for *ERF6*, which was in cluster 35 (Figure S1A).

After recovery, about 57% of HL upregulated genes were downregulated and 66% of HL downregulated genes were upregulated (Figure S1B; Table S2). When using 2-fold change as the criterion, 79% of HL72h DEGs restored their expression to the non-stress level while the rest (21%) could not (Figure S1C). For example, the expression of *RHL41* restored to the non-stress level after recovery. *AT1G12030* did not express under GL, was highly induced by HL, and recovered to the moderate expression level after recovery. The opposite expression pattern was observed for *LHCB2.2* (Figure S1D).

To our knowledge, most previous studies describing the HL-related transcriptomes only had one or two time points and did not exclude the interference of heat. We compared our DEGs with those identified in previous studies. We found that 85% of DEGs in Kleine et al. (2007), 36% of DEGs in Jung et al. (2013), 59% of DEGs in Suzuki et al. (2015), and 42% of DEGs in Crisp et al. (2017) were observed in our study. We also found that more than 70% of our HL DEGs were not identified in previous studies and some previously reported DEGs did not appear in our data (Figure S2A). Previous studies showed that many heat shock factor (*HSF*) and *HSP* genes, including *HSFA2*, *HSP70*, *HSP17.6A*, *HSP18.2*, and *HSP21*, were highly induced by short-time HL (Crisp et al., 2017). However, in our data, HSP18.2 did not show differential expression under HL, while *HSP70*, *HSP17.6A*, and *HSP21* were uninduced or lowly induced under 0.5 and 6 h of HL treatment (Figure 2E; Table S2). We confirmed this observation by qPCR (Figures 2F-2J) and found that most of these *HSF* and *HSP* genes were only highly induced by warm HL. These results indicated that the induction of these *HSF* and *HSP* genes under short-time HL treatment was heat driven.

We also compared our data with transcriptomes of other abiotic stresses, including heat (Higashi et al., 2015) and drought (Crisp et al., 2017). We found that only 16% of the genes were common between HL and heat and 30% of the genes were shared by HL and drought (Figure S2B). For these three stresses, 226 genes were common DEGs, and their enriched Gene Ontology (GO) terms were mainly related to stress response (Figure S2C).

The Set of Core HL Stress-Responsive Genes

Of the 5,403 DEGs, 250 genes were differentially expressed across all six HL time points (Figure 3A; Table S4A). These 250 common genes appeared to be the core HL-responsive genes. The expression pattern of these genes clustered into three groups. Genes in group I had dramatically decreased expression, expression of group II genes showed a moderate increase of less than 5-fold, and expression of group III genes increased dramatically (Figure 3B). Among the 250 common genes, in addition to known HL-responsive genes (e.g., *ELIP1*, *ELIP2*, *GPT2*, and *RHL41*), we found some highly induced genes (e.g., *ELI3-2*, *AT1G71000*, and *BAM5*) and severely repressed genes (e.g., *BBX17*, *SAUR3*, and *SAUR27*). Moreover, five genes were from the *B box* (*BBX*) gene family, which has 32 members (Khanna et al., 2009), and nine genes were from the *SMALL AUXIN UPREGULATED RNA* (*SAUR*) gene family, which has 80 members (Markakis et al., 2013). BBXs can act as negative or positive regulators of light signaling (Huang et al., 2012). Four of the five *BBX* genes were downregulated at all six time points, while *BBX31* was upregulated (Figure 3C). We also found that BBX31 was the upstream regulator of *ELIP2* based on the *Arabidopsis* cistrome data (O'Malley et al., 2016) (Figure 3D). Our data also showed that 18 *BBX* genes were regulated by HL (Figure 3C; Table S4B). All nine *SAUR* genes were downregulated from 0.5 to 72 h of HL. Moreover, 46 *SAUR* genes were differentially expressed for at least one HL time point (Figure 3E; Table S4B).

We then constructed a co-expression network of the 250 common DEGs (Figure S3A). We first extracted the sub-network using *RHL41* as the seed gene, which was involved in the HL stress response (lida et al., 2000; Rossel et al., 2007). *RHL41* had 67 connections in the co-expression network. Besides *ELIP1* and *ELIP2*, *BBX17*, *BBX27*, *SAUR15*, *SAUR27*, and *SAUR29* co-expressed with *RHL41* (Figure S3B). The top three hub genes that had the highest degree and betweenness centrality in the co-expression network were *AT1G27210*, *AT4G01330*, and *BBX14* (Figure S3A). *AT1G27210*, a member of the ARM repeat superfamily, had 129 connections (Figure 4A). *AT4G01330* is a protein kinase gene and had 124 connections (Figure 4B). *BBX14* had 112 connections (Figure 4C). All three hub genes were co-expressed with *ELIP1*, *ELIP2*, and *GPT2*, suggesting that these genes were potentially important HL response regulators. We acquired the mutants of *AT1G27210* and *AT4G01330* and assayed their phenotypes under HL. We found that after about 20 h of HL, *AT1G27210* mutants had more plants with bleached, paler cotyledons and less chlorophyll content compared with the wild type, suggesting that this hub gene might play an important role in HL stress response (Figures S3C and S3D).

Gene Ontology (GO) Term Enrichment of HL Differentially Expressed Genes

To gain insight into biological processes in response to HL, we analyzed the GO term enrichment of DEGs of different HL time points. For HL upregulated DEGs, GO terms

related to stress and stimulus response were significantly enriched for all time points. GO terms related to high light intensity, light intensity, response to light stimulus, UV, and UV-B were also enriched. Hormone-related GO terms, e.g., response to abscisic acid (ABA), jasmonic acid (JA), auxin, salicylic acid (SA) stimulus, or mediated signaling pathway, were enriched. In addition, anthocyanin and flavonoid metabolic process were enriched after 6 h of HL (Figure S4A; Table S5). For downregulated DEGs, stress and light response-related GO terms were enriched, and photosynthesis-related terms appeared after 6 h of HL. The GO term enrichments for long-term HL (24, 48, and 72 h) were similar and included development-related GO terms, e.g., cell differentiation, cell wall modification, trichoblast differentiation, epidermis, ectoderm, and root development. Moreover, terms related to growth and development hormones brassinosteroids (BRs), auxin, and cytokinin showed up (Figure S4B; Table S5). The enriched GO terms for the 0.5 h DEGs were different from those of other time points; e.g., GO terms related to gene expression, RNA biosynthetic, RNA elongation, and RNA metabolic only appeared for 0.5 h. Altogether, this analysis suggests that HL significantly regulates the expression of genes involved in stress stimulus, light response, hormone, anthocyanin metabolism, photosynthesis, and development. Of interest, the top GO terms for upregulated DEGs of recovery were the GO terms for the downregulated DEGs of 24, 48, and 72 h, and vice versa (Figure S4; Table S5).

Hormone Biosynthetic and Signaling Pathways Are Involved in HL Stress Response

To inspect the role of hormones in different durations of HL stress response, we analyzed the expression changes of biosynthetic genes for different phytohormones. Most genes in ABA and JA biosynthetic pathways showed increased expression at all time points. SA, ethylene, and gibberellic acid (GA) biosynthetic genes only showed significant expression changes at a few time points (Figure 5A). We identified nine DEGs from the ABA biosynthetic genes, including *NCED3*, *NCED5*, and *NCED9*, which were upregulated after 0.5 h of HL, and *NCED2*, which had increased expression only after 24 h of HL. Four *CYP707* genes involved in the oxidative catabolism of ABA were upregulated under HL (Table S6). In addition, ABA signaling pathway genes were regulated by HL (Figure 5B). Six of the 14 ABA receptor genes were HL DEGs, and most of them were downregulated after HL. Eight of the nine clade A *PP2C* genes were persistently upregulated by HL (Figure 5B). We measured the ABA levels in plants under GL or HL at each time point. The ABA level increased slightly after 0.5 h of HL, dramatically increased by more than 2-fold after 6 h of HL, and then maintained at a high level for the entire duration of HL. The ABA level decreased during recovery but was still higher than GL control (Figure 5C). To validate the role of ABA in HL, and because *NCED3* was differentially expressed across all six HL time points, we investigated the phenotype of ABA biosynthesis-defective mutant *nced3nced5*. After 24 h of HL, the *nced3nced5* mutants were hypersensitive to HL; more mutant plants had bleached cotyledons with larger bleached areas compared with the wild type (Figure 5D). To quantify the phenotype, we found that *nced3nced5* mutants had less chlorophyll content compared with the wild type under HL (Figure 5E), which suggests that ABA is required for HL stress response.

Twelve of 17 JA biosynthetic genes were differentially expressed. Seven of nine SA biosynthetic genes were DEGs, and nine of 12 ethylene biosynthetic genes were

differentially expressed for at least one time point (Table S6). Of the 24 GA biosynthetic genes, 11 were differentially expressed for at least one time point (Table S6). BRs, auxin, and cytokinin are known to regulate many aspects of plant development, and many of their biosynthetic genes showed changes in transcript abundance in response to HL (Figure 5A). BR biosynthetic pathway genes showed repressed expression at all time points, while genes involved in auxin and cytokinin biosynthesis showed decreased expression under long-term HL. Three of the BR biosynthetic genes were downregulated from short- to long-term HL, while *UGT73C5*, which is responsible for BL-23-O-glucosylation, was upregulated across all HL time points (Table S6). Fourteen of the 32 genes involved in auxin biosynthesis were DEGs, of which 10 were downregulated for at least one time point (Table S6). Seven of 10 cytokinin biosynthetic genes were downregulated for at least one time point. The downregulation of genes involved in hormones related to plant growth and development correlates with the observation that plant growth is retarded under HL stress. In addition, JA, GA, BR, auxin, and cytokinin signaling pathway genes were regulated by HL (Figure S5).

The Genes for Blue/UV-A Receptors and PIFs Are Responsive to HL Stress

We asked whether genes for photoreceptors and phytochrome-interacting factors (PIFs) were responsive to high-intensity light-driven signaling. We analyzed the expression of genes for red/far-red photoreceptors (*PHYA*, *PHYB*, *PHYC*, *PHYD*, and *PHYE*), blue/UV-A photoreceptors (*CRY1*, *CRY2*, *PHOT1*, *PHOT2*, *ZTL*, *FKF1*, and *LKP2*), the UV-B receptor (*UVR8*), and *PIFs* (including *PIF1*, *PIF3*, *PIF4*, *PIF5*, and *PIF7*). The expression levels of *PHYA* to *PHYE* were similar between GL and HL (Table S1). However, *CRY1* and *PHOT1* were downregulated after HL, and *FKF1* showed rapid upregulation followed by downregulation (Figure 6A). The similar expression pattern for blue/UV-A photoreceptor genes under HL may explain the synergistic relationships of different receptors in acclimation to HL. Cryptochromes interact with UVR8 and are required for plant survival in natural and simulated sunlight (Rai et al., 2019). We then compared the HL DEGs with UV-B-regulated genes and found that 58% (778 of 1,349) of UV-B-regulated genes (Favory et al., 2009) were also differentially expressed under our HL treatment (Figure S6A).

We found that *PIF1*, *PIF4*, *PIF5*, and *PIF7* genes were all downregulated by HL (Figure 6B). To investigate the role of *PIF* genes in HL stress response, we examined the phenotype of *pif1*, *pif4*, *pif5*, *pif7*, *pif4*,*5*, and the quadruple mutant *pif1*,*3*,*4*,*5* (*pifq*). After 24 h of HL, *pif4*, *pif5*, *pif4*,*5*, and *pifq* mutants showed HL-hypersensitive phenotypes; the mutants had more plants with bleached cotyledons, and the bleached areas in cotyledons of mutant plants were larger compared with the wild type (Figure 6C). We found that *pif4*, *pif5*, *pif4*,*5*, and *pifq* mutants had less chlorophyll content compared with the wild type under HL (Figure 6D). We compared the HL DEGs with *PIFQ*-regulated genes (Zhang et al., 2013) and found that 44% (891 of 2,025) of *pifq*-regulated genes were differentially expressed under HL (Figure S6B), which supported the important role of *PIFs* in HL stress response.

PIFs are the key regulators in shade-avoidance responses (Lorrain et al., 2008; Li et al., 2012). Shade also increases the endogenous ABA level, probably by enhancing the transcript level of ABA biosynthetic genes *NCED3* and *NCED5* (Kohnen et al., 2016). After we observed that *NCED3/5* and *PIFs* were required for HL stress response, and to determine the

link between *NCED3/5* and *PIFs* under HL, we examined the expression of *NCED* genes in *pifq* mutants before and after HL treatment. The results showed that the induction of *NCED3* and *NCED5* by HL were similar between wild-type and *pifq* mutants (Figure S6C), suggesting that the induction of *NCED3/5* by HL was independent of *PIFs*.

Genes Encoding the Photosynthetic Apparatus Respond to Middle- to Long-Term HL

Our data showed that the expression of most photosystem genes changed little after 0.5 h of HL. However, these genes were dramatically repressed after 6 h of HL, indicating an adjustment in the light harvesting system and reaction centers to capture less light energy for photosynthesis. Eleven nucleus-encoded genes in Photosystem I were downregulated from 6 to 72 h of HL and upregulated after recovery (Figure 7A). In Photosystem II, the expression of *PsbP1*, *PsbO1*, *PsbQ1*, and *PsbQ2* was downregulated (Figure 7A). The expression of genes encoding Light harvesting complex I (LHCI) proteins, including *Lhca1*, *Lhca2.1*, *Lhca3*, and *Lhca4*, was also repressed after HL (Figure 7A). Transcript levels of 13 of the 16 genes encoding Light harvesting complex II (LHCII) proteins were reduced under HL (Figure 7A). The expression of *PPL1* and *PnsL4* was downregulated more than 2-fold at 48 h of HL. The transcript levels of other component genes in the electron flow chain, including the cytochrome b6f complex, ferredoxin, and the cyclic electron flow switch, were similar to control, except *petM* and *ferredoxin 2* were suppressed since 48 h of HL, *PC1* was downregulated from 6 to 48 h, and *PC2* was downregulated at 24 and 48 h of HL (Table S6). In contrast, most genes involved in the Calvin-Benson cycle did not change their expression. This suggests that HL is more harmful to light reaction than the Calvin-Benson cycle (Table S6).

Consistent with the downregulation of plant growth-related hormone genes and photosynthetic genes, after 24 h of HL, the fresh weight of HL-treated plants was significantly lower compared with control, indicating that the growth of plants was inhibited by long-term HL (Figure 7B).

Anthocyanin Biosynthetic Genes Are Activated after 6 h of HL Treatment

Under HL, *Arabidopsis* plants accumulate anthocyanin in vegetative tissues, which can act as sunscreen, protecting cells from photoinhibition and damage by absorbing blue-green and UV light. We analyzed the expression profile of anthocyanin biosynthetic genes (Solfanelli et al., 2006). Anthocyanin biosynthesis can be divided into three phases: the general phenylpropanoid pathway, the flavonoid pathway, and the anthocyanin-specific pathway (Shi and Xie, 2014). PAL1, C4H, and 4CL proteins are involved in the beginning steps of these pathways, and six of their corresponding genes were DEGs. *PAL3* was downregulated since 0.5 h of HL, and the rest of the genes were upregulated after 6 h of HL (Figure 7C; Table S6). Chalcone synthase, chalcone isomerase, and flavanone 3-hydroxylase (F3H) carry out the initial steps of the flavonoid pathway. Five genes encoding these enzymes were upregulated after 6 h of HL and maintained a high expression level in long-term HL. Three *MYB* transcription factor genes (*MYB11*, *MYB12*, and *MYB111*) were upregulated across all six time points (Figure 7D; Table S6). The late steps transform dihydroflavonols into anthocyanidins and modify the anthocyanidins. Eighteen genes involved in these steps were differentially expressed (Figure 7E; Table S6). The anthocyanin content significantly

increased after 12 h of HL and continuously accumulated with HL treatment time lapse. After recovery, the anthocyanin content decreased but was still higher than that of non-treatment control (Figure 7F).

DISCUSSION

Plants in the natural environment have to cope with climate changes and different stresses on timescales ranging from seconds to months, including HL stress. Heat is the most common confounded stress in HL stress response studies. By controlling the leaf and medium temperatures in our experiment design, we were able to exclude the interference of heat in HL stress response. Indeed, less heat-responsive genes were identified as DEGs in our data. In contrast to previously reported strong induction by HL, *HSP* and *HSF* genes, as well as *APX2*, were only slightly upregulated under our HL conditions (Figures 1 and 2), which emphasizes the importance of discerning the specific action and biological consequences of high-intensity light-driven stress response by our study. The high temporal resolution of our time course data uncovers the relative dynamics of transcriptional changes and at which time point each differentially expressed gene first showed a significant change, along with the magnitude and duration of that change. Plants seem to have different transcriptional responses to different timescales of HL stress, especially by dynamic regulation of different hormone biosynthesis, signaling, photosynthesis, and anthocyanin pathway genes. Our data also indicated that during recovery, the expression of about 79% of the HL DEGs recovered to the non-stress level and the rest did not recover to the non-stress level (Figure S1). These non-fully recovered genes may play a role in HL acclimation and the HL stress memory of plants.

Compared with related transcriptome studies, our study has identified a large number of different HL-responsive genes. There are several possible explanations for this observation: (1) Our study encompassed HL treatment over a 72-h period, while previous studies looked at only short treatment periods. (2) Plants were at different stages of development when subjected to HL. Both Kleine et al. (2007) and our study looked at the effects of HL on 7-day-old seedlings, and these data were most similar. (3) We have eliminated heat as a variable in our experiment, which allows us to uncover the specific high-intensity light-driven transcriptome. Furthermore, comparing with heat and drought transcriptome, a large portion of DEGs exclusively respond to each stress (Figure S2), which means different transcription-regulation mechanisms are likely used by plants to deal with different abiotic stresses.

Our results suggested that plants may respond to HL through the dynamic metabolism of different phytohormones, e.g., ABA, JA, and SA, which have been suggested to be involved in light acclimation (Ramel et al., 2013; Suzuki et al., 2013; Dietz, 2015). For the short term, ABA might be a signal for triggering response to HL (Galvez-Valdivieso et al., 2009; Suzuki et al., 2013). The continuous high level of ABA content during different durations of HL and the HL-hypersensitive phenotype of *nced3nced5* double mutants (Figures 5D and 5E) further suggest the important role of ABA in middle- and long-term HL stress response. It was reported that JA was associated with HL-induced cell death (Ramel et al., 2013). Consistent with this, we observed that most JA biosynthetic genes were upregulated at all time points.

The role of SA in HL has also been established by using mutants disturbing SA levels (Mateo et al., 2006). However, we found that BR biosynthetic genes were downregulated by HL, which might suggest the negative role of BR in HL stress response. The almost opposite regulation of the ABA and BR biosynthetic genes might correlate with the antagonistic relationship of gene expression levels between ABA and BRs displayed in several physiological responses (Zhou et al., 2014). In addition, under long-term HL, the expression of growth-related hormones' biosynthetic genes was repressed, which was consistent with the observation that plant development and growth were inhibited by long-term HL. The complexity underlying expression of these genes illustrates the extraordinary interconnectedness of the signaling pathways regulated by phytohormones in response to HL stress.

Our analysis also provides strong support for aspects of the transcriptome regulated by HL that had not been firmly established and identifies additional players in this pathway. Overall, 250 genes were differentially expressed across all time points of HL treatment, thus defining a set of core *Arabidopsis* HL-responsive genes, including many *BBX* and *SAUR* genes. We demonstrated that more than half of the *BBX* genes were differentially expressed for at least one time point. BBX31, whose gene was strongly induced by HL, was the upstream regulator of HL marker gene *ELIP2* (Figures 3C and 3D). It was reported that BBX31 acts as a negative regulator of photomorphogenesis under light (Heng et al., 2019; Yadav et al., 2019) but a positive regulator of UV-B signaling (Yadav et al., 2019). The HL spectrum showed that the light source in our study also contains a low dose of UV-B. Moreover, *BBX31* positively regulates *ELIP1* and *ELIP2* gene expression in a UV-B-dependent manner (Yadav et al., 2019), which supports the function of BBX31 in HL stress response. *BBX14* is one of the hub genes in the co-expression network. Moreover, *BBX14*, *BBX15*, and *BBX17*, which were repressed at all time points, and *BBX16*, which was downregulated starting from 6 h of HL, were in the same small clade of the *BBX* phylogenetic tree (Khanna et al., 2009). The BBXs in this clade contains one B box and one CCT domain, and this small clade may have a potential role in HL response through light signaling. *SAUR* genes regulate plant cell expansion, shade avoidance, tropic growth, apical hook development, leaf growth, and senescence (Ren and Gray, 2015). The regulation of more than half of the *SAUR* genes by HL may be related to the auxin level and may contribute to the plants' retarded growth phenotype under HL. These *BBX* and *SAUR* genes identified in our analysis are good candidates for future functional validation studies.

Although the UV-B receptor *UVR8* is not a DEG under HL, more than half of the UV-B-regulated genes were differentially expressed under our HL treatment (Figure S6A). We infer that UVR8 proteins may be altered under our HL treatment. *PIFs* are central regulators that integrate multiple internal and external signals to optimize plant development (Leivar and Monte, 2014). *PIF4* is a central integrator in the transcriptional network regulating plant high-temperature response (Quint et al., 2016; Li et al., 2018). We show that *PIF4* plays the most prominent role in HL stress response, with an additional role played by *PIF5*. *PIF1* and *PIF3* are proposed as negative regulators controlling chloroplast development (Huq et al., 2004; Stephenson et al., 2009). Although *PIF1* was a differentially expressed gene under HL (Figure 6B; Table S1), the *pif1* mutant assembled the phenotype of the wild type under HL. G box is the dominant binding site of *PIFs* (Zhang et al., 2013; Pfeiffer et al., 2014) and

enriched in the promoters of HL DEGs (Figure 2C). Therefore, our study uncovers the role of *PIFs* in HL stress response.

Altogether, we propose a hypothesis of how plants respond to different durations of HL stress through light-driven transcriptional networks. In this hypothesis, after exposure to HL for a short time, plants start to activate pathways functioning in stress response, like ABA and JA biosynthesis, while repressing the nucleotide metabolic and BR biosynthetic processes. After middle-term HL, anthocyanin starts to accumulate and genes for photosynthesis are repressed. After long-term HL, the growth of plants is affected and the biosynthesis of growth-related hormones like auxin and cytokinin is suppressed. However, plants can recover from long-term HL in a relatively short time (Figure S7). The data provided here reveal a genome-wide and dynamic transcriptional landscape of high-intensity light-driven stress response in *Arabidopsis*, which furthers our knowledge of how plants respond to HL stress and provides a powerful resource and candidates for evaluating the involvement of genes in HL stress response. Our study also provides a resource for comparative transcriptome analysis of different stresses in plants.

STAR★METHODS

LEAD CONTACT AND MATERIALS AVAILABILITY

Further information and requests for resources should be directed to and will be fulfilled by the Lead Contact, Joanne Chory (chory@salk.edu). This study did not generate new unique reagents.

EXPERIMENTAL MODEL AND SUBJECT DETAILS

Plant Material and Growth Conditions—The *Arabidopsis thaliana* ecotype Columbia (*Col-0*) is the wild-type. The *pif1* (Lee et al., 2015), *pif4* (Lorrain et al., 2008), *pif5* (Lorrain et al., 2008), *pif4,5* (Lorrain et al., 2008), *pifq* (Leivar et al., 2008a), *pif7-1* (Leivar et al., 2008b), and *nced3nced5* (Frey et al., 2012) mutants were described previously. T-DNA insertion mutants for *AT1G27210* (*SALK_015125C*) and *AT4G01330* (*SALK_107777C*) were ordered from ABRC. Seeds were surface sterilized using chlorine gas for four hours and plated on 1/2LS medium, pH 5.7 (Caisson Laboratories, UT, USA), with 0.8% micropropagation type-1 agar (Caisson Laboratories). After 4-day stratification in the dark at 4°C, plants were grown under 60 μmol m^{-2} s^{-1}, 24 h constant light at 22°C. After seven days, half of the plates were treated with continuous 1200 μmol m^{-2} s^{-1} high light in Conviron E8 chamber. The spectra of HL is measured by the Spectroradiometer SPR-03 (Luzchem) and the detailed spectra of HL is UV-A (315 - 400 nm) 18.7 μmol m^{-2} s^{-1}, UV-B (280 - 315nm) 1.3 μmol m^{-2} s^{-1}, UV-C (200 - 280 nm)1.1 μmol m^{-2} s^{-1}, Blue light (400-499 nm) 172 μmol m^{-2} s^{-1}, Red light (600 - 699 nm) 799 μmol m^{-2} s^{-1}, and FR light (700 - 799 nm) 596 μmol m^{-2} s^{-1}. We used an Etekcity Lasergrip 630 Dual Laser Non-contact Digital Infrared Thermometer to monitor the medium and plant leaf temperatures. The high light chamber was set to 11.5°C because of the cool air came from the bottom of the chamber to make sure the medium and leaf temperatures were kept at 22°C to match the control growth condition. Samples were harvested at 0.5 h, 6 h, 12 h, 24 h, 48 h, and 72 h high light treatment time point and recovery samples were collected after 14 h recovery in

normal growth condition following 72 h HL. The rest plates were kept in the 60 μmol m^{-2} s^{-1}, 22°C chamber for collecting control samples at each time point. For each time point, 25 seedlings were collected as one sample and two biological replicates were collected.

METHOD DETAILS

Total RNA Exaction and RNA-Seq Library Preparation—Total RNA was extracted using the RNeasy Plant Mini Kit (QIAGEN) with dsDNase treated following the manufacturer's instruction. The RNA concentration was measured using Qubit® 2.0 Fluorometer (Invitrogen). 4 μg total RNA was used to prepare RNA-seq libraries using the TruSeq Stranded mRNA Library Prep Kit (Illumina, San Diego, US). Single-end sequencing was performed on Illumina HiSeq 2500 sequencing machine at the Next-Generation Sequencing Core of the Salk Institute for Biological Studies.

Identification and Analysis of Differentially Expressed Genes—BRB Digital Gene Expression (BRB-DGE) tool (https://arraytools.github.io/bdge/) was used to get the raw counts of each gene. Briefly, RNA-seq reads were aligned to the *Arabidopsis* reference genome (TAIR10) using TopHat version 2.1.1 (Kim et al., 2013) and gene-level raw count data files were generated using HTSeq version 0.6.0 (Anders et al., 2015). The raw count data were imported into Bioconductor package edgeR (Robinson et al., 2010) in the R language to identify the differentially expressed genes and to calculate the RPKM of each gene. When calculating the differentially expressed genes, a gene was retained only if it was expressed at a count-per-million (CPM) above 0.5 in at least two samples. Those genes had a log2-converted fold change ≥ 1 or ≤ −1 with an FDR (False Discovery Rate) ≤ 0.05 were considered as DEGs. The organelle transcripts were excluded in further analyses. All DEGs cluster analysis was detected by Short Time-series Expression Miner (STEM) software with the maximum number of model profile set to 40 (Ernst and Bar-Joseph, 2006). Motif discovery was performed using the MEME version 5.0.5 (Bailey and Elkan, 1994).

Co-expression Analysis and Analysis of Enriched GO Terms—The co-expression networks were constructed using the Pearson correlation coefficient (Contreras-López et al., 2018) and visualized using Cytoscape (Shannon et al., 2003). The Venn diagrams were generated using interactivenn (http://www.interactivenn.net/) (Heberle et al., 2015) or using http://bioinformatics.psb.ugent.be/webtools/Venn/ and modified manually. Gene ontology (GO) enrichment analysis was determined using agriGO (Du et al., 2010). Genes of hormone biosynthetic pathways were obtained from the website of the RIKEN (http://hormones.psc.riken.jp/pathway_hormones.html). The photosystem genes list was according to Sun et al. (2013).

Anthocyanin Measurement—Growth light or high light treated seedlings were harvested, weighed, and ground in liquid nitrogen to the fine powder. Anthocyanin measurements were performed as described (Neff and Chory, 1998). Briefly, the pigments were extracted in methanol with 1% HCl. Water was added and the chlorophyll was extracted with an equal volume of chloroform. Total anthocyanin was determined by measuring the A530 and A657 of the aqueous phase by using a spectrophotometer (DU-730,

Beckman). Quantification of anthocyanins was performed using the following equation: Anthocyanin contents = (A530 - 0.25*A657)/weight.

ABA Measurement—Growth light or HL treated seedlings were harvested, weighed, and ground in liquid nitrogen to the fine powder. The ABA measurements were carried out at Salk institute mass spectrometry core according to (Owen and Abrams, 2009).

Chlorophyll Content Measurement—Plants were grown under GL (60 μmol m^{-2} s^{-1}, 24 h constant light at 22°C) for 8 days for GL samples or under GL for 7 days then treated with HL (1200 μmol m^{-2} s^{-1}, leaf temperature 22°C) for 24 h for HL samples. Chlorophyll content measurement was performed as described previously (Zhao et al., 2018) with modifications. In brief, GL or HL treated seedlings were harvested, weighed, and ground in liquid nitrogen to the fine powder. Chlorophyll was extracted in 1 mL 80% acetone (v/v %) and the cell debris was removed by centrifugation at 10,000 g for 15 min at 4°C. Chlorophyll was measured spectrophotometrically and levels were calculated according to the formula provided in the previous study (Lichtenthaler and Wellburn, 1983).

Quantitative Real-Time PCR (qPCR)—Wild-type plant (*Col-0*) were grown under GL condition (60 μmol m^{-2} s^{-1}) for 7d at 22°C then treated with different high light conditions (HL chamber was set to 11.5°C or 22°C) for 6 h, followed by collection and RNA extraction. Total RNA was extracted using RNeasy Plant Mini Kit (QIAGEN), and the first-strand cDNA was synthesized using Maxima First Strand cDNA Synthesis with dsDNase Kit for RT-qPCR (Thermo) following the manual. qPCR was performed on a CFX384 Real-Time PCR Detection System using iTaq Universal SYBR® Green Supermix (Bio-rad). The PCR cycling condition consisted of an initial 3 min at 95°C followed by 44 cycles of 10 s at 95°C, 30 s at 60°C and 30 s at 72°C. Data were analyzed with Bio-Rad CFX Manager software (Version 1.6). The primers used for qPCR were listed in Table S7.

Mutant Genotyping—Homozygous T-DNA insertion mutant lines were identified using mutant gene-specific primers and T-DNA left-border primer: LBb1.3. The primers were listed in Table S7. PCR was carried out using the OneTaq® 2 × Master Mix with Standard Buffer (NEB). The following thermal condition was used: 94°C for 5 min, 35 cycles of 94°C for 30 s, 55°C for 45 s, 72°C for 1 min.

QUANTIFICATION AND STATISTICAL ANALYSIS

Significant differences between two samples were determined with Student’s t test. Significant differences for multiple comparisons were determined by one-way or two-way ANOVA as indicated in figure legends. The plots and heatmaps were generated using R (https://www.r-project.org/). Technical and biological replicate experiments were performed as indicated.

DATA AND CODE AVAILABILITY

The RNA-seq raw data in this paper were deposited into the National Center for Biotechnology Information (NCBI) Gene Expression Omnibus database under accession number GEO: GSE111062.

Supplementary Material

Refer to Web version on PubMed Central for supplementary material.

ACKNOWLEDGMENTS

This work was supported by the Howard Hughes Medical Institute, the NIH (grant R35GM122604 to J.C.), and the U.S. Department of Energy (grant DE-FG02-04ER15540 to J.C.). X.Z. is partially supported by the Hundred Talents Program of Zhejiang University. RNA-seq and ABA measurement were performed at the Next-Generation Sequencing Core and Mass Spectrometry Core of the Salk Institute for Biological Studies, respectively (funding from NIH-NCI CCSG, P30 014195; the Chapman Foundation; the Helmsley Charitable Trust; and the Helmsley Center for Genomic Medicine). We thank Dr. Adam Seluzicki for text editing and discussion, Dr. Ullas Pedmale for suggestions on RNA sequencing, Dr. Antonio Michel Pinto for technical support, and Dr. Yogev Burko, Dr. Björn C. Willige, and Dr. Po-Kai Hsu for providing the *pif* and *nced3nced5* seeds.

REFERENCES

Anders S, Pyl PT, and Huber W (2015). HTSeq—a Python framework to work with high-throughput sequencing data. Bioinformatics 31, 166–169. [PubMed: 25260700]

Apel K, and Hirt H (2004). Reactive oxygen species: metabolism, oxidative stress, and signal transduction. Annu. Rev. Plant Biol 55, 373–399. [PubMed: 15377225]

Athanasiou K, Dyson BC, Webster RE, and Johnson GN (2010). Dynamic acclimation of photosynthesis increases plant fitness in changing environments. Plant Physiol. 152, 366–373. [PubMed: 19939944]

Bailey TL, and Elkan C (1994). Fitting a mixture model by expectation maximization to discover motifs in biopolymers. Proc. Int. Conf. Intell. Syst. Mol. Biol 2, 28–36. [PubMed: 7584402]

Casazza AP, Rossini S, Rosso MG, and Soave C (2005). Mutational and expression analysis of *ELIP1* and *ELIP2* in *Arabidopsis thaliana*. Plant Mol. Biol 58, 41–51. [PubMed: 16028115]

Contreras-López O, Moyano TC, Soto DC, and Gutiérrez RA (2018). Step-by-step construction of gene co-expression networks from high-throughput *Arabidopsis* RNA sequencing data. Methods Mol. Biol 1761, 275–301. [PubMed: 29525965]

Crisp PA, Ganguly DR, Smith AB, Murray KD, Estavillo GM, Searle I, Ford E, Bogdanović O, Lister R, Borevitz JO, et al. (2017). Rapid recovery gene downregulation during excess-light stress and recovery in *Arabidopsis*. Plant Cell 29, 1836–1863. [PubMed: 28705956]

Dietz K-J (2015). Efficient high light acclimation involves rapid processes at multiple mechanistic levels. J. Exp. Bot 66, 2401–2414. [PubMed: 25573858]

Du Z, Zhou X, Ling Y, Zhang Z, and Su Z (2010). agriGO: a GO analysis toolkit for the agricultural community. Nucleic Acids Res. 38, W64–W70. [PubMed: 20435677]

Ernst J, and Bar-Joseph Z (2006). STEM: a tool for the analysis of short time series gene expression data. BMC Bioinformatics 7, 191. [PubMed: 16597342]

Favory J-J, Stec A, Gruber H, Rizzini L, Oravecz A, Funk M, Albert A, Cloix C, Jenkins GI, Oakeley EJ, et al. (2009). Interaction of COP1 and UVR8 regulates UV-B-induced photomorphogenesis and stress acclimation in *Arabidopsis*. EMBO J. 28, 591–601. [PubMed: 19165148]

Frey A, Effroy D, Lefebvre V, Seo M, Perreau F, Berger A, Sechet J, To A, North HM, and Marion-Poll A (2012). Epoxycarotenoid cleavage by NCED5 fine-tunes ABA accumulation and affects seed dormancy and drought tolerance with other NCED family members. Plant J. 70, 501–512. [PubMed: 22171989]

Galvez-Valdivieso G, Fryer MJ, Lawson T, Slattery K, Truman W, Smirnoff N, Asami T, Davies WJ, Jones AM, Baker NR, and Mullineaux PM (2009). The high light response in *Arabidopsis* involves ABA signaling between vascular and bundle sheath cells. Plant Cell 21, 2143–2162. [PubMed: 19638476]

Goss R, and Lepetit B (2015). Biodiversity of NPQ. J. Plant Physiol 172, 13–32. [PubMed: 24854581]

Heberle H, Meirelles GV, da Silva FR, Telles GP, and Minghim R (2015). InteractiVenn: a web-based tool for the analysis of sets through Venn diagrams. BMC Bioinformatics 16, 169. [PubMed: 25994840]

Heddad M, Norén H, Reiser V, Dunaeva M, Andersson B, and Adamska I (2006). Differential expression and localization of early light-induced proteins in *Arabidopsis*. Plant Physiol. 142, 75–87. [PubMed: 16829586]

Heng Y, Lin F, Jiang Y, Ding M, Yan T, Lan H, Zhou H, Zhao X, Xu D, and Deng XW (2019). B-box containing proteins BBX30 and BBX31, acting downstream of HY5, negatively regulate photomorphogenesis in *Arabidopsis*. Plant Physiol. 180, 497–508. [PubMed: 30765480]

Higashi Y, Okazaki Y, Myouga F, Shinozaki K, and Saito K (2015). Landscape of the lipidome and transcriptome under heat stress in *Arabidopsis thaliana*. Sci. Rep 5, 10533. [PubMed: 26013835]

Huang J, Zhao X, Weng X, Wang L, and Xie W (2012). The rice B-box zinc finger gene family: genomic identification, characterization, expression profiling and diurnal analysis. PLoS ONE 7, e48242. [PubMed: 23118960]

Huq E, Al-Sady B, Hudson M, Kim C, Apel K, and Quail PH (2004). Phytochrome-interacting factor 1 is a critical bHLH regulator of chlorophyll biosynthesis. Science 305, 1937–1941. [PubMed: 15448264]

Iida A, Kazuoka T, Torikai S, Kikuchi H, and Oeda K (2000).A zinc finger protein RHL41 mediates the light acclimatization response in *Arabidopsis*. Plant J. 24, 191–203. [PubMed: 11069694]

Jiao Y, Lau OS, and Deng XW (2007). Light-regulated transcriptional networks in higher plants. Nat. Rev. Genet 8, 217–230. [PubMed: 17304247]

Jung H-S, Crisp PA, Estavillo GM, Cole B, Hong F, Mockler TC, Pogson BJ, and Chory J (2013). Subset of heat-shock transcription factors required for the early response of *Arabidopsis* to excess light. Proc. Natl. Acad. Sci. USA 110, 14474–14479. [PubMed: 23918368]

Kaiserli E, Páldi K, O'Donnell L, Batalov O, Pedmale UV, Nusinow DA, Kay SA, and Chory J (2015). Integration of light and photoperiodic signaling in transcriptional nuclear foci. Dev. Cell 35, 311–321. [PubMed: 26555051]

Kasahara M, Kagawa T, Oikawa K, Suetsugu N, Miyao M, and Wada M (2002). Chloroplast avoidance movement reduces photodamage in plants. Nature 420, 829–832. [PubMed: 12490952]

Khanna R, Kronmiller B, Maszle DR, Coupland G, Holm M, Mizuno T, and Wu S-H (2009). The *Arabidopsis* B-box zinc finger family. Plant Cell 21, 3416–3420. [PubMed: 19920209]

Kim G-T, Yano S, Kozuka T, and Tsukaya H (2005). Photomorphogenesis of leaves: shade-avoidance and differentiation of sun and shade leaves. Photochem. Photobiol. Sci 4, 770–774. [PubMed: 16121290]

Kim D, Pertea G, Trapnell C, Pimentel H, Kelley R, and Salzberg SL (2013). TopHat2: accurate alignment of transcriptomes in the presence of insertions, deletions and gene fusions. Genome Biol. 14, R36. [PubMed: 23618408]

Kleine T, Kindgren P, Benedict C, Hendrickson L, and Strand A (2007). Genome-wide gene expression analysis reveals a critical role for CRYPTO-CHROME1 in the response of *Arabidopsis* to high irradiance. Plant Physiol. 144, 1391–1406. [PubMed: 17478635]

Knapp A, and Carter G (1998). Variability in leaf optical properties among 26 species from a broad range of habitats. Am. J. Bot 85, 940. [PubMed: 21684977]

Kohnen MV, Schmid-Siegert E, Trevisan M, Petrolati LA, Sénéchal F, Müller-Moulé P, Maloof J, Xenarios I, and Fankhauser C (2016). Neighbor detection induces organ-specific transcriptomes, revealing patterns underlying hypocotyl-specific growth. Plant Cell 28, 2889–2904. [PubMed: 27923878]

Lee N, Park J, Kim K, and Choi G (2015). The transcriptional coregulator LEUNIG_HOMOLOG inhibits light-dependent seed germination in *Arabidopsis*. Plant Cell 27, 2301–2313. [PubMed: 26276832]

Leivar P, and Monte E (2014). PIFs: systems integrators in plant development. Plant Cell 26, 56–78. [PubMed: 24481072]

Leivar P, Monte E, Oka Y, Liu T, Carle C, Castillon A, Huq E, and Quail PH (2008a). Multiple phytochrome-interacting bHLH transcription factors repress premature seedling photomorphogenesis in darkness. Curr. Biol 18, 1815–1823. [PubMed: 19062289]

Leivar P, Monte E, Al-Sady B, Carle C, Storer A, Alonso JM, Ecker JR, and Quail PH (2008b). The *Arabidopsis* phytochrome-interacting factor PIF7, together with PIF3 and PIF4, regulates

responses to prolonged red light by modulating phyB levels. Plant Cell 20, 337–352. [PubMed: 18252845]

Li L, Ljung K, Breton G, Schmitz RJ, Pruneda-Paz J, Cowing-Zitron C, Cole BJ, Ivans LJ, Pedmale UV, Jung H-S, et al. (2012). Linking photoreceptor excitation to changes in plant architecture. Genes Dev. 26, 785–790. [PubMed: 22508725]

Li B, Gao K, Ren H, and Tang W (2018). Molecular mechanisms governing plant responses to high temperatures. J. Integr. Plant Biol 60, 757–779. [PubMed: 30030890]

Lichtenthaler HK, and Wellburn AR (1983). Determinations of total carotenoids and chlorophylls a and b of leaf extracts in different solvents. Biochem. Soc. Trans 11, 591–592.

Lorrain S, Allen T, Duek PD, Whitelam GC, and Fankhauser C (2008). Phytochrome-mediated inhibition of shade avoidance involves degradation of growth-promoting bHLH transcription factors. Plant J. 53, 312–323. [PubMed: 18047474]

Markakis MN, Boron AK, Van Loock B, Saini K, Cirera S, Verbelen J-P, and Vissenberg K (2013). Characterization of a small auxin-up RNA (SAUR)-like gene involved in *Arabidopsis thaliana* development. PLoS ONE 8, e82596. [PubMed: 24312429]

Mateo A, Funck D, Mühlenbock P, Kular B, Mullineaux PM, and Karpinski S (2006). Controlled levels of salicylic acid are required for optimal photosynthesis and redox homeostasis. J. Exp. Bot 57, 1795–1807. [PubMed: 16698814]

Mishra Y, Jänkänpää HJ, Kiss AZ, Funk C, Schróder WP, and Jansson S (2012). *Arabidopsis* plants grown in the field and climate chambers significantly differ in leaf morphology and photosystem components. BMC Plant Biol. 12, 6. [PubMed: 22236032]

Neff MM, and Chory J (1998). Genetic interactions between phytochrome A, phytochrome B, and cryptochrome 1 during *Arabidopsis* development. Plant Physiol. 118, 27–35. [PubMed: 9733523]

O'Malley RC, Huang SC, Song L, Lewsey MG, Bartlett A, Nery JR, Galli M, Gallavotti A, and Ecker JR (2016). Cistrome and epicistrome features shape the regulatory DNA landscape. Cell 165, 1280–1292. [PubMed: 27203113]

Owen SJ, and Abrams SR (2009). Measurement of plant hormones by liquid chromatography-mass spectrometry. Methods Mol. Biol 495, 39–51. [PubMed: 19085148]

Pfeiffer A, Shi H, Tepperman JM, Zhang Y, and Quail PH (2014). Combinatorial complexity in a transcriptionally centered signaling hub in *Arabidopsis*. Mol. Plant 7, 1598–1618. [PubMed: 25122696]

Quint M, Delker C, Franklin KA, Wigge PA, Halliday KJ, and van Zanten M (2016). Molecular and genetic control of plant thermomorphogenesis. Nat. Plants 2, 15190. [PubMed: 27250752]

Rai N, Neugart S, Yan Y, Wang F, Siipola SM, Lindfors AV, Winkler JB, Albert A, Brosché M, Lehto T, et al. (2019). How do cryptochromes and UVR8 interact in natural and simulated sunlight? J. Exp. Bot 70, 4975–4990. [PubMed: 31100755]

Ramel F, Ksas B, Akkari E, Mialoundama AS, Monnet F, Krieger-Liszkay A, Ravanat J-L, Mueller MJ, Bouvier F, and Havaux M (2013). Light-induced acclimation of the *Arabidopsis chlorina1* mutant to singlet oxygen. Plant Cell 25, 1445–1462. [PubMed: 23590883]

Ren H, and Gray WM (2015). SAUR proteins as effectors of hormonal and environmental signals in plant growth. Mol. Plant 8, 1153–1164. [PubMed: 25983207]

Robinson MD, McCarthy DJ, and Smyth GK (2010). edgeR: a Bioconductor package for differential expression analysis of digital gene expression data. Bioinformatics 26, 139–140. [PubMed: 19910308]

Rossel JB, Wilson IW, and Pogson BJ (2002). Global changes in gene expression in response to high light in *Arabidopsis*. Plant Physiol. 130, 1109–1120. [PubMed: 12427978]

Rossel JB, Wilson PB, Hussain D, Woo NS, Gordon MJ, Mewett OP, Howell KA, Whelan J, Kazan K, and Pogson BJ (2007). Systemic and intracellular responses to photooxidative stress in *Arabidopsis*. Plant Cell 19, 4091–4110. [PubMed: 18156220]

Ruban AV (2016). Nonphotochemical chlorophyll fluorescence quenching: mechanism and effectiveness in protecting plants from photodamage. Plant Physiol. 170, 1903–1916. [PubMed: 26864015]

Schöttler MA, and Tóth SZ (2014). Photosynthetic complex stoichiometry dynamics in higher plants: environmental acclimation and photosynthetic flux control. Front. Plant Sci 5, 188. [PubMed: 24860580]

Shannon P, Markiel A, Ozier O, Baliga NS, Wang JT, Ramage D, Amin N, Schwikowski B, and Ideker T (2003). Cytoscape: a software environment for integrated models of biomolecular interaction networks. Genome Res. 13, 2498–2504. [PubMed: 14597658]

Shi M-Z, and Xie D-Y (2014). Biosynthesis and metabolic engineering of anthocyanins in *Arabidopsis thaliana*. Recent Pat. Biotechnol 8, 47–60. [PubMed: 24354533]

Solfanelli C, Poggi A, Loreti E, Alpi A, and Perata P (2006). Sucrose-specific induction of the anthocyanin biosynthetic pathway in *Arabidopsis*. Plant Physiol. 140, 637–646. [PubMed: 16384906]

Stephenson PG, Fankhauser C, and Terry MJ (2009). PIF3 is a repressor of chloroplast development. Proc. Natl. Acad. Sci. USA 106, 7654–7659. [PubMed: 19380736]

Sun F, Liang C, Whelan J, Yang J, Zhang P, and Lim BL (2013). Global transcriptome analysis of *AtPAP2*—overexpressing *Arabidopsis thaliana* with elevated ATP. BMC Genomics 14, 752. [PubMed: 24180234]

Suzuki N, Miller G, Salazar C, Mondal HA, Shulaev E, Cortes DF, Shuman JL, Luo X, Shah J, Schlauch K, et al. (2013). Temporal-spatial interaction between reactive oxygen species and abscisic acid regulates rapid systemic acclimation in plants. Plant Cell 25, 3553–3569. [PubMed: 24038652]

Suzuki N, Devireddy AR, Inupakutika MA, Baxter A, Miller G, Song L, Shulaev E, Azad RK, Shulaev V, and Mittler R (2015). Ultra-fast alterations in mRNA levels uncover multiple players in light stress acclimation in plants. Plant J. 84, 760–772. [PubMed: 26408339]

Vogel MO, Moore M, König K, Pecher P, Alsharafa K, Lee J, and Dietz K-J (2014). Fast retrograde signaling in response to high light involves metabolite export, MITOGEN-ACTIVATED PROTEIN KINASE6, and AP2/ERF transcription factors in *Arabidopsis*. Plant Cell 26, 1151–1165. [PubMed: 24668746]

Wada M (2013). Chloroplast movement. Plant Sci. 210, 177–182. [PubMed: 23849124]

Walters RG (2005). Towards an understanding of photosynthetic acclimation. J. Exp. Bot 56, 435–447. [PubMed: 15642715]

Wookey PA, Parsons AN, Welker JM, Potter JA, Callaghan TV, Lee JA, and Press MC (1993). Comparative responses of phenology and reproductive development to simulated environmental change in sub-arctic and high arctic plants. Oikos 67 (3), 490–502.

Yadav A, Bakshi S, Yadukrishnan P, Lingwan M, Dolde U, Wenkel S, Masakapalli SK, and Datta S (2019). The B-box-containing microprotein miP1a/BBX31 regulates photomorphogenesis and UV-B protection. Plant Physiol. 179, 1876–1892. [PubMed: 30723178]

Zhang Y, Mayba O, Pfeiffer A, Shi H, Tepperman JM, Speed TP, and Quail PH (2013). A quartet of PIF bHLH factors provides a transcriptionally centered signaling hub that regulates seedling morphogenesis through differential expression-patterning of shared target genes in *Arabidopsis*. PLoS Genet. 9, e1003244. [PubMed: 23382695]

Zhao X, Huang J, and Chory J (2018). *genome uncoupled1* mutants are hypersensitive to norflurazon and lincomycin. Plant Physiol. 178, 960–964. [PubMed: 30154176]

Zhou J, Wang J, Li X, Xia X-J, Zhou Y-H, Shi K, Chen Z, and Yu J-Q (2014). H_2O_2 mediates the crosstalk of brassinosteroid and abscisic acid in tomato responses to heat and oxidative stresses. J. Exp. Bot 65, 4371–4383. [PubMed: 24899077]

Highlights

- The specific transcriptome of plants under high-intensity light without heat stress
- Different durations of HL stress cause dynamic changes to the transcriptome
- Hormone, photosynthetic, and anthocyanin genes are dynamically regulated by HL
- *nced3nced5* and *pif* mutants are hypersensitive to high light

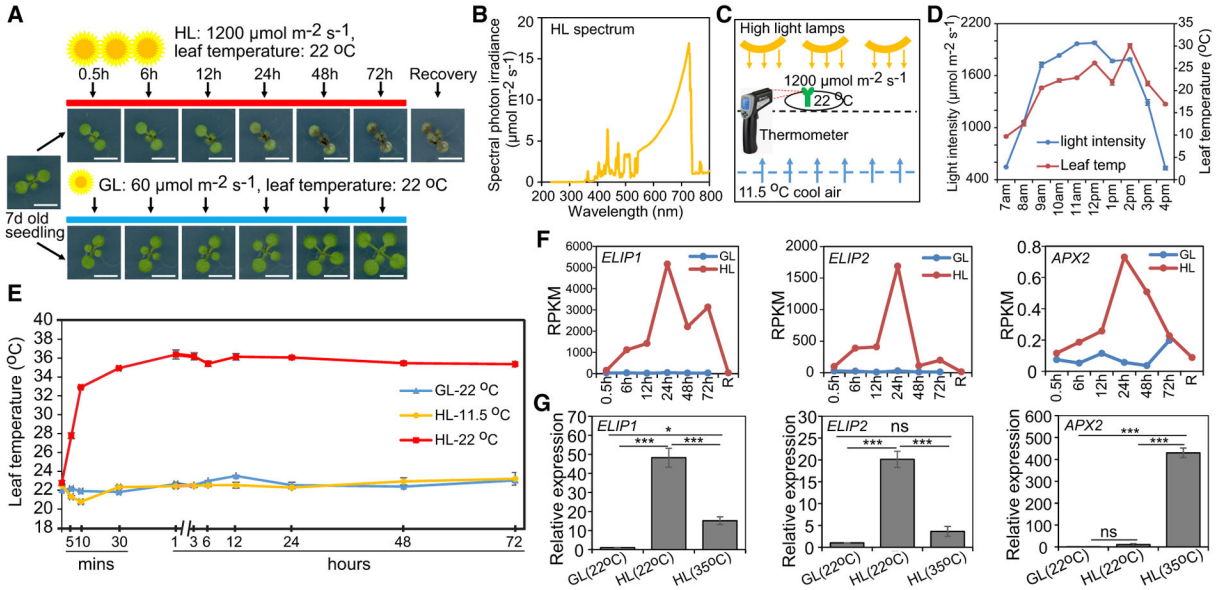

Figure 1. Time Course HL Stress Response and Recovery Experimental Design and HL Marker Gene Expression Patterns

(A) The experimental scheme for time course RNA-seq analysis of plants under HL. Arrows indicate plants at the time points of HL treatment. Scale bar is 1 cm.

(B) The spectrum of HL. The x axis is the wavelength. The y axis is the spectral photon irradiance level.

(C) The schematic diagram of the HL chamber setup.

(D) The measurement of light intensity and leaf temperature on December 7, 2018 (sunrise: 6:38 AM, sunset: 4:42 PM, weather forecast: sunny, 10°C to 18°C) around the Salk Institute for Biological Studies.

(E) The measurement of leaf temperature during HL treatment. GL-22°C represents growth light (GL: 60 μmol m^{-2} s^{-1}, temperature setting: 22°C). HL-11.5°C represents high light and lower temperature (HL: 1,200 μmol m^{-2} s^{-1}, temperature setting: 11.5°C), and HL-22°C represents high light and higher temperature (1,200 μmol m^{-2} s^{-1}, temperature setting: 22°C).

(F) The expression level of HL marker genes under GL and HL from RNA-seq data. The x axis indicates the time points. The y axis represents the average RPKM.

(G) The qPCR analysis of *ELIP1*, *ELIP2*, and *APX2* expression under different HL conditions for 6 h. The x axis indicates different conditions. GL (22°C), GL with a leaf temperature of 22°C; HL (22°C), HL with a leaf temperature of 22°C; HL (35°C), HL with a leaf temperature of 35°C. The y axis represents the relative expression level, and the expression level of GL (22°C) is set as 1. Values are mean ± SEM of three biological replicates. Asterisks represent significant differences (*$p < 0.05$, ***$p < 0.001$) determined by one-way ANOVA followed by Tukey's HSD (honestly significant difference) comparisons. ns, not significant.

See also Table S1.

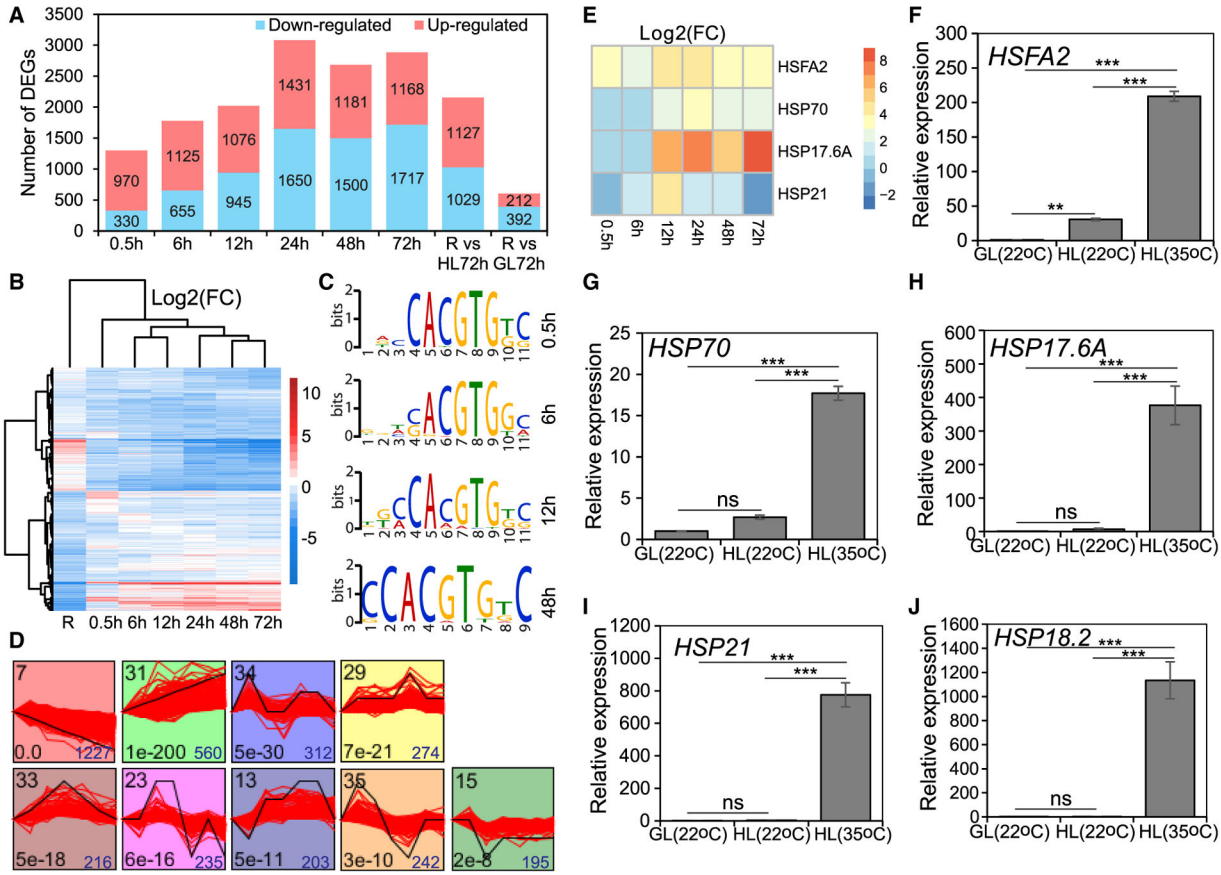

Figure 2. Global Transcriptome Response of the Plant to HL Stress and Recovery, as well as the Expression Pattern of Selected *HSF* and *HSP* Genes

(A) The number of DEGs at each time point and recovery (R).

(B) The heatmap shows the expression profile of all DEGs. The heatmap is clustering the log2 fold change (log2(FC)) of each gene.

(C) The enrichment of G box motifs in the promoters of differentially expressed genes. The x axis represents the conserved sequences of the motif. The y axis is a scale of the relative entropy, which reflects the conservation rate of each nucleic acid. Time points are labeled on the right.

(D) Nine significant expression clusters ($p < 0.05$) of all DEGs. The p value and DEG number of each cluster are shown in the left and right bottom corners in each panel, respectively. The cluster names are showed in the left top corner.

(E) The heatmap shows the expression profile of selected *HSF* and *HSP* genes under HL from RNA-seq. Log2(FC), log2 fold change.

(F–J) The qPCR analysis of selected *HSF* and *HSP* gene expression under different HL conditions for 6 h. The x axis indicates the different conditions. The labels of different conditions are the same as in Figure 1G. The y axis is the relative expression level, and the expression level of GL (22°C) is set as 1. Values are mean ± SEM of three biological replicates. Asterisks represent significant differences (**$p < 0.01$, ***$p < 0.001$) determined by one-way ANOVA followed by Tukey's HSD comparisons. ns, not significant. The

corresponding gene for each panel is: (F): *HSFA2*; (G): *HSP70*; (H): *HSP17.6A*; (I): *HSP21*; and (J): *HSP18.2.*

See also Figures S1 and S2 and Tables S2 and S3.

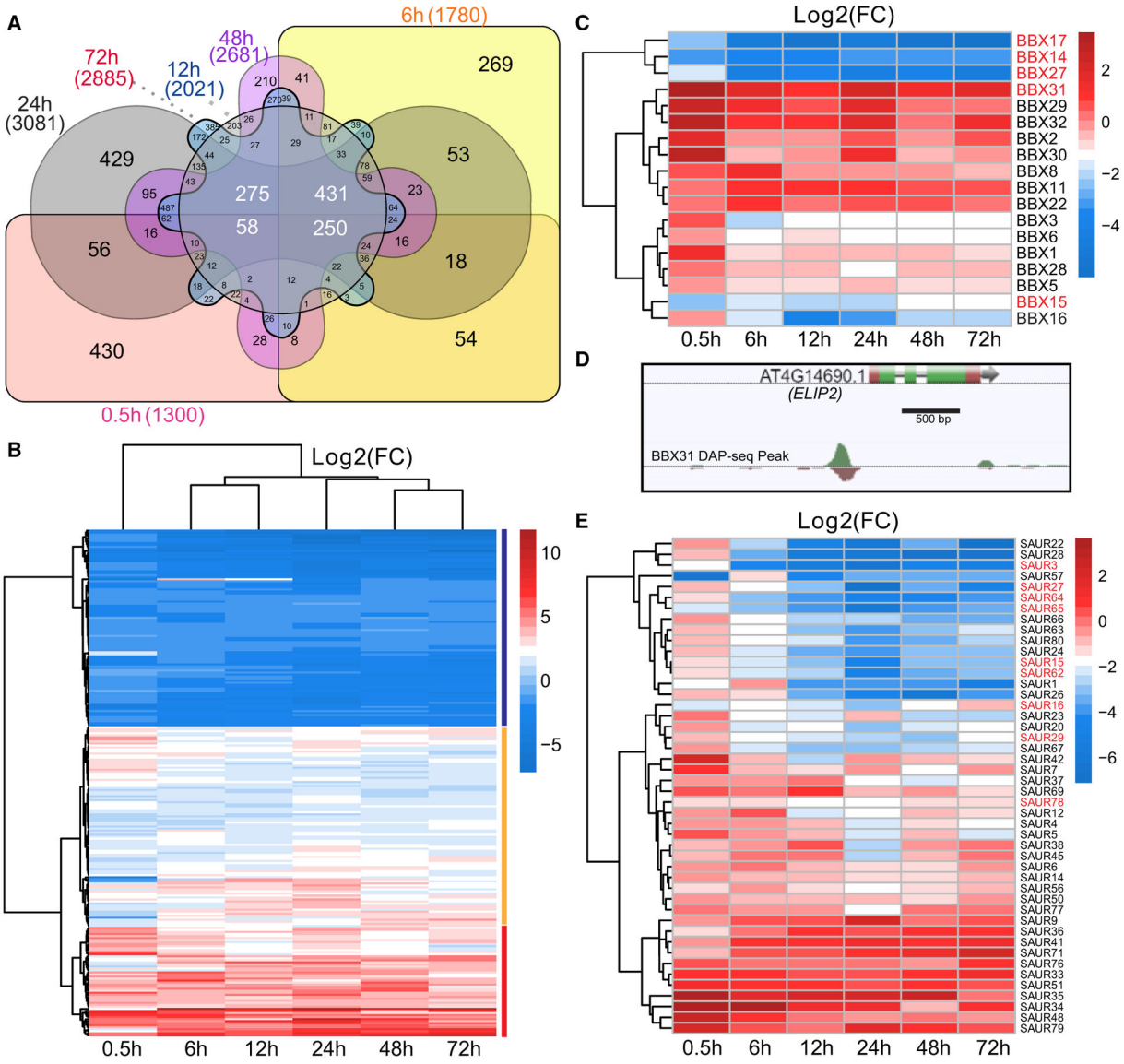

Figure 3. The Expression Profile of the 250 Common DEGs and *BBX* and *SAUR* Genes across All Six HL Time Points

(A) The Venn diagram displays the overlap of DEGs for the HL time points.

(B) The heatmap shows the expression pattern of the 250 common DEGs. Three expression groups are marked, with blue, orange, and red lines representing groups I, II, and III, respectively. Log2(FC), log2 fold change.

(C) The heatmap shows the expression profile of differentially expressed *BBX* genes for six HL time points. The five *BBX* genes marked in red are differentially expressed at all six time points. Log2(FC), log2 fold change.

(D) The DAP-seq (DNA affinity purification sequencing) data (from O'Malley et al., 2016) show the binding of BBX31 to the promoter of *ELIP2*.

(E) The heatmap shows the expression profile of differentially expressed *SAUR* genes for six HL time points. The nine *SAUR* genes marked in red have differential expression at all six time points. Log2(FC), log2 fold change.

See also Table S4.

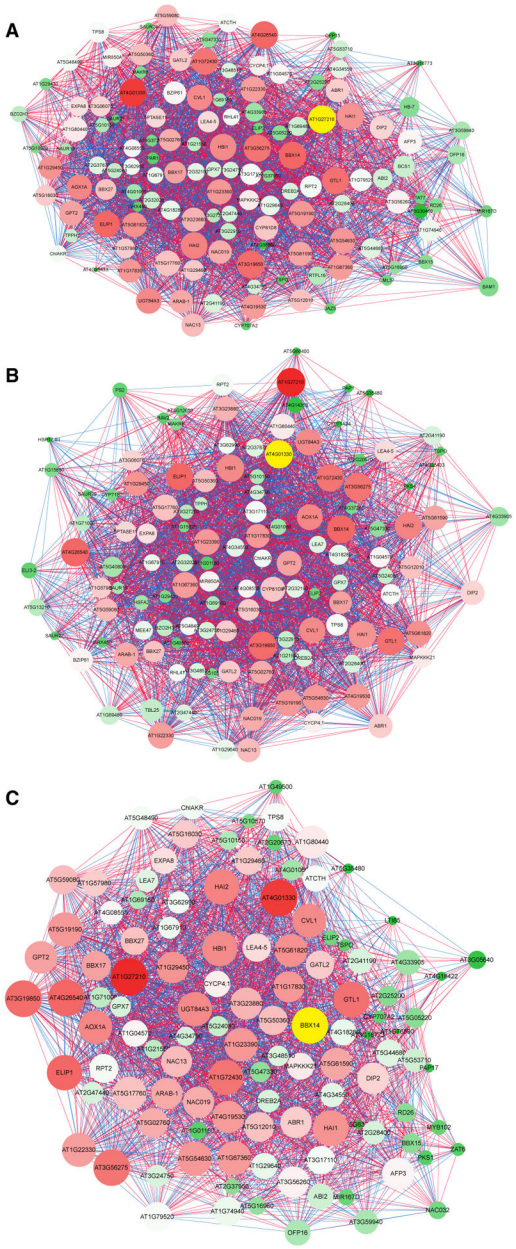

Figure 4. The Co-expression Sub-networks of the HL Response Hub Genes

The color of each gene is based on degree and betweenness centrality. The genes in red suggest highly connected nodes or hub genes, whereas the genes in green are less connected nodes. The seed gene is marked in yellow. The red and blue lines between genes represent positive and negative correlations, respectively.

(A) The sub-network of hub gene *AT1G27210.*

(B) The sub-network of hub gene *AT4G01330.*

(C) The sub-network of hub gene *BBX14.*

See also Figure S3.

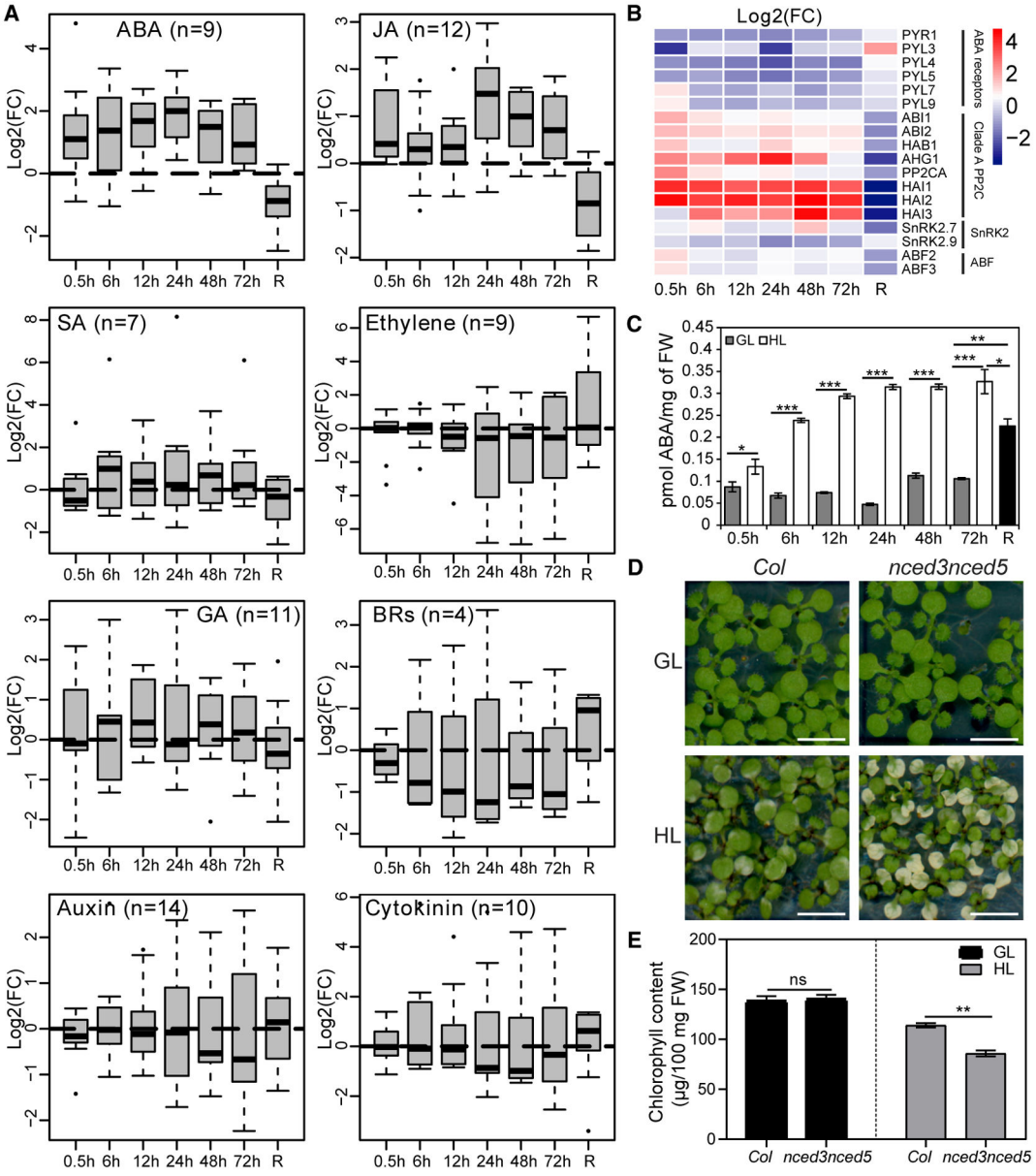

Figure 5. Hormone Biosynthetic Pathway Genes Are Dynamically Regulated by HL

(A) The boxplots show the expression profile of DEGs that are involved in hormone biosynthetic pathways under HL. The horizontal black dash line is the zero line of log2 fold change. Black lines in the boxes indicate the mean fold change. The x axis is the time point of HL and recovery (R). The y axis is log2 fold change (log2(FC)).

(B) The heatmap shows the expression profile of DEGs involved in the ABA signaling pathway.

(C) The ABA level under GL or HL at each time point and recovery. Values are mean ± SEM of two biological replicates. Asterisks indicate significant differences (*$p < 0.05$, ***$p < 0.001$) between GL and HL as determined by two-way ANOVA followed by Bonferroni multiple comparisons. The significant differences (*$p < 0.05$, **$p < 0.01$, ***$p < 0.001$) between R and HL or GL are determined by Student's t test.

(D) The phenotype of *nced3nced5* double mutants under GL and HL. Plants were grown under GL (60 μmol m^{-2} s^{-2}, 24 h of constant light at 22°C) for 7 days and then treated with HL (1,200 μmol m^{-2} s^{-1}, leaf temperature: 22°C) for 24 h. Scale bar is 5 mm.
(E) The chlorophyll content differences between wild-type *Col* and *nced3nced5* double mutants. The y axis is the chlorophyll content. Data are mean ± SEM (three biological replicates). Asterisks indicate Student's t test significant differences (**$p < 0.01$). ns, not significant.
See also Figures S4, S5, and S7 and Table S6.

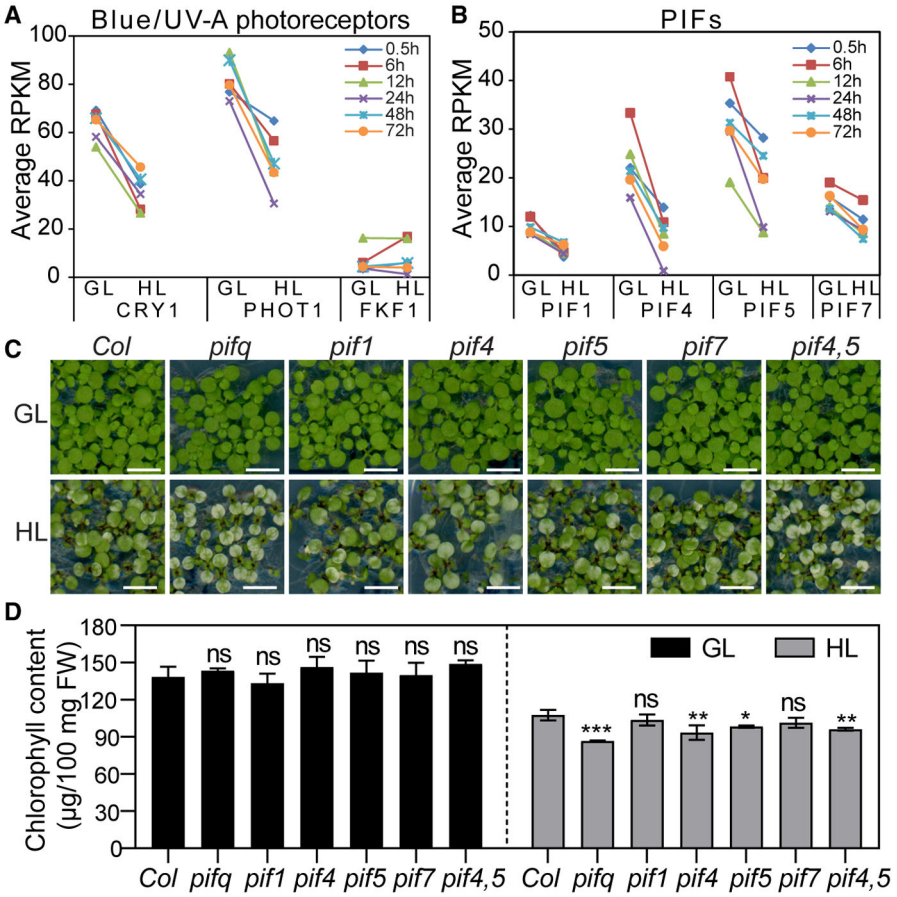

Figure 6. Genes for Blue/UV-A Photoreceptors and PIFs Are Regulated by HL

(A) The expression pattern of blue/UV-A photoreceptor genes under HL. The x axis indicates the names of the genes and treatment. The y axis represents the average RPKM.

(B) The expression pattern of *PIFs* under HL. The x axis indicates the genes and treatment. The y axis is the average RPKM.

(C) The phenotype of *pif* mutants under GL and HL. Plants were grown and treated with HL as indicated in Figure 5D. Scale bar is 5 mm.

(D) The chlorophyll content differences between *Col* and mutant plants. The y axis is the chlorophyll content. Data are mean ± SEM (three biological replicates). Asterisks indicate significant differences (*p < 0.05, **p < 0.01, ***p < 0.001) between mutants and the wild type under the same condition as determined by one-way ANOVA followed by Dunnett's multiple comparisons, ns, not significant.

See also Figures S6 and S7 and Table S1.

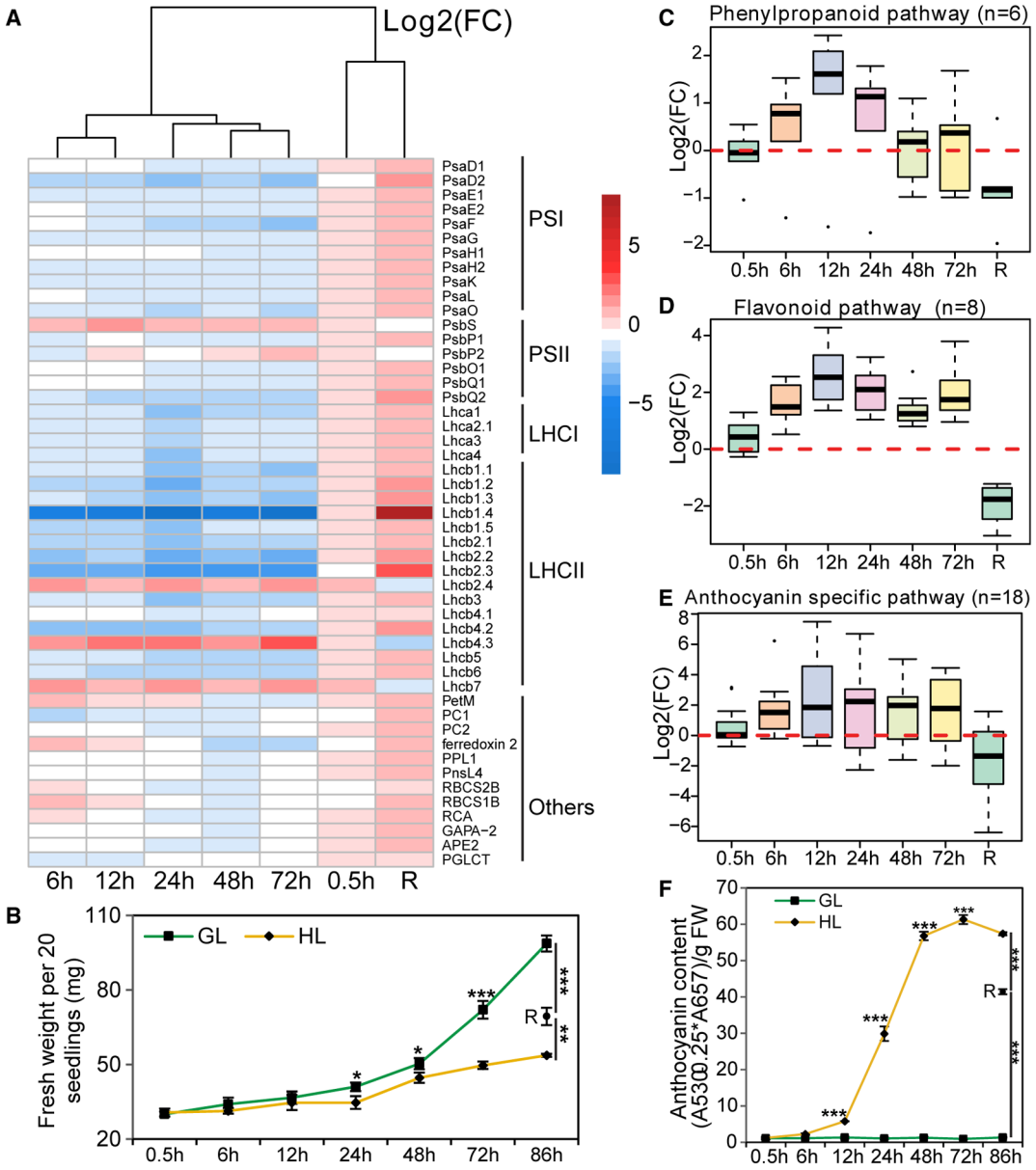

Figure 7. Photosynthetic and Anthocyanin Biosynthetic Genes and Plant Growth Are Regulated by HL

(A) The heatmap shows the expression pattern of photosynthetic genes. Genes from PSI, PSII, LHCI, and LHCII are marked on the right.

(B) The fresh weight of plants under HL and recovery. Asterisks indicate significance (*$p < 0.05$, **$p < 0.01$, ***$p < 0.001$) determined by two-way ANOVA followed by Bonferroni multiple comparisons (three biological replicates, $n = 20$).

(C–E) The expression profile of genes involved in the beginning steps of the general phenylpropanoid pathway (C), early steps of the flavonoid pathway (D), and late steps of the anthocyanin-specific pathway (E). The x axis is the time point of HL. The y axis represents log2(FC).

(F) The anthocyanin content under HL and recovery. Asterisks indicate significance (***$p < 0.001$) determined by two-way ANOVA followed by Bonferroni multiple comparisons (three biological replicates).

See also Figure S7 and Table S6.

KEY RESOURCES TABLE

REAGENT or RESOURCE	SOURCE	IDENTIFIER
Chemicals, Peptides, and Recombinant Proteins		
Methanol	Fisher	A412-4
Hydrochloric acid	EMD Millipore	HX0603-75
Actone	Fisher	A946-4
Linsmaier & Skoog with Buffer Medium	Caisson Laboratories	LSP03-1LT
Micropropagation agar type-1	Caisson Laboratories	A038-500GM
Critical Commercial Assays		
RNeasy Plant Mini Kit	QIAGEN	74904
RNase-Free DNase Set	QIAGEN	79254
TruSeq Stranded mRNA Library Prep Kit	Illumina	20020594
Maxima First Strand cDNA Synthesis Kit for RT-qPCR, with dsDNase	Thermo	K1671
iTaq Universal SYBR® Green Supermix	Bio-rad	1725121
OneTaq® 2 × Master Mix with Standard Buffer	NEB	M0482S
Deposited Data		
Raw RNA-Seq data from *Arabidopsis*	This paper	GEO: GSE111062
Experimental Models: Organisms/Strains		
Arabidopsis: *Col-0*	N/A	N/A
Arabidopsis: *SALK_015125C*	ABRC	*SALK_015125C*
Arabidopsis: *SALK_107777C*	ABRC	*SALK_107777C*
Arabidopsis: *nced3nced5*	Frey et al., 2012	N/A
Arabidopsis: *pif1*	Lee et al., 2015	SALK_131872
Arabidopsis: *pif7*	Leivar et al., 2008b	N/A
Arabidopsis: *pif4*, *pif5*, *pif4,5*	Lorrain et al., 2008	N/A
Arabidopsis: *pif1,3,4,5* (*pifq*)	Leivar et al., 2008a	N/A
Software and Algorithms		
R package (version 2.3.4)	https://www.r-project.org/	N/A
BRB Digital Gene Expression (BRB-DGE) tool	https://arraytools.github.io/bdge/	N/A
TopHat version 2.1.1	Kim et al., 2013	https://ccb.jhu.edu/software/tophat/index.shtml
HTSeq version 0.6.0	Anders et al., 2015	https://htseq.readthedocs.io/en/release_0.11.1/
edgeR	Robinson et al., 2010	https://bioconductor.org/packages/release/bioc/html/edgeR.html
Short Time-series Expression Miner (STEM)	Ernst and Bar-Joseph, 2006	http://www.cs.cmu.edu/~jernst/stem/
Co-expression networks	Contreras-López et al., 2018	N/A
Cytoscape	Shannon et al., 2003	https://cytoscape.org
Interactivenn	Heberle et al., 2015	http://www.interactivenn.net/
Other		
Conviron E8 chamber	Conviron	N/A
Etekcity Lasergrip 630 dual laser non-contact digital infrared thermometer	Etekcity	N/A

REAGENT or RESOURCE	SOURCE	IDENTIFIER
Spectrophotometer (DU-730)	Beckman	DU-730
Light Meter	LI-COR	LI-250A
Spectroradiometer	Luzchem	SPR-03
CFX384 Real-Time PCR Detection System	Bio-rad	184-5384